



Sulfamic acid heterogenized on hydroxyapatite-encapsulated γ -Fe₂O₃ nanoparticles as a magnetic green interphase catalyst

Mehdi Sheykhan^a, Leila Ma'mani^b, Ali Ebrahimi^a, Akbar Heydari^{a,*}

^a Chemistry Department, Tarbiat Modares University, P.O. Box 14155-4838, Tehran, Iran

^b Department of Medicinal Chemistry, Faculty of Pharmacy and Pharmaceutical Sciences Research Center, Tehran University, Iran

ARTICLE INFO

Article history:

Received 18 October 2010

Received in revised form 6 December 2010

Accepted 8 December 2010

Available online 17 December 2010

Dedicated to memory of Noor Ali Shooshtari.

Keywords:

Catalysis

Immobilization

Inorganic–organic hybrid

Magnetic recovery

Sulfamic acid

Magnetic core

ABSTRACT

A highly efficient and green system is introduced to chemical synthesis. Magnetic nanoparticle-supported propylsulfamic acid deposited onto hydroxyapatite [γ -Fe₂O₃-HAP-(CH₂)₃-NH₂SO₃H] synthesized as a unique heterogeneous acid catalyst of excellent activity and recyclable for at least 10 reaction runs without significant loss of activity. The facile recovery of the catalyst is carried out by applying an external magnet device. It is both “green” and efficient. The catalyst was fully characterized by spectroscopic, magnetic, adsorptive and thermal techniques (TEM, SEM, FTIR, TGA, XRD, BET, elemental analysis (CHNOS) and VSM).

© 2010 Elsevier B.V. All rights reserved.

1. Introduction

Following the successful applications of magnetic nanoparticles in designing of new catalytic supports [1], there is now a growing interest in the further development of this type of catalyst supports. So, magnetic catalytic systems have been introduced as vastly powerful and clean recoverable supports for a variety of catalytic reactions. The use from nano-particles as catalyst has some problems. One of them is their high active surface which leads to the agglomeration of the catalyst particles. Coating the catalyst surface with an organic or an inorganic shell is an appropriate strategy to prevent agglomeration [2–7]. Hydroxyapatite has been demonstrated to be preferable in terms of versatility in surface modification, thermal and chemical stability and biocompatibility as one of the ideal materials for encapsulation of iron oxide nanoparticles [8,9]. A general trend in catalysis is to convert a homogeneous catalyst into a heterogeneous catalytic system [10–22]. The immobilization of homogeneous catalysts on solid supports opens up new avenues for design and engineering of new and stimulating catalysts. These structures are easily separable from the reaction mixture, allowing the recov-

ery of the solid and eventually its reuse. The highest level of evolution in the surface immobilization strategy is the covalent attachment of the organic compound or ligand to the solid surface [23]. While immobilizing a homogeneous catalyst on a surface, diffusion of the reactants to the catalyst site may take place with difficulty [24], resulting in decreased catalytic activity. To overcome this problem and enhance the availability of the active catalyst sites, materials with porous structures such as zeolites have been utilized [25–29] or by other procedures, smaller sized particles of catalyst were produced [3]. The incorporation of organic moieties with pendant attached chains, either on the external part or on the internal surface, is an applicable modifying manner to change the physical and chemical properties of natural or synthesized materials. It can improve the ability of the new multifunctional materials – considered as “inorganic–organic hybrids” – to act in a variety of academic or technological activities [30]. An obvious advantage of such hybrids is the favorable combination of both organic and inorganic properties in one nanomaterial [31]. The inorganic–organic hybrids can combine the novel inorganic properties like mechanical, thermal or structural stability as well as the organic features such as tendency toward water, leakage from water, reactivity and also can be modified of bulk characteristics such as mechanical and optical properties (by the designing different organo-functionalization onto the surface) [32].

* Corresponding author. Tel.: +98 21 82883444; fax: +98 21 82883455.
E-mail address: akbar.heydari@gmx.de (A. Heydari).

With respect to their high selectivity, resulting from the extended surface, the usage of catalysts supported on nano structural has been increasing [33]. The extended surface (caused by the nanosized structure) also improves the loading of the catalyst during immobilization process [34]. In other words, as the particle size decreases filtration becomes increasingly more difficult. Therefore, despite many advantages, catalyst recovery remains as challenge. Thus some of the drawbacks of the traditional procedures are the tedious recycling via lengthy filtration and the inevitable loss of solid catalyst during the separation process [35–37]. Receive to the green aspect requires the use of a more effective recovery method for these types of catalysts.

Among various magnetic nanoparticles, γ -Fe₂O₃ (maghemite), owing to its good thermal and chemical stability coated with hydroxyapatite, has been considered as an ideal candidate. It has a high surface area, surface modification ability, easily synthesized, low toxicity and an important biocompatible inorganic catalyst support [38]. Hydroxyapatite-encapsulated magnetic γ -Fe₂O₃ [γ -Fe₂O₃@HAp] nanocrystallinities have been recently used as a high-performance heterogeneous catalytic supports [33]. On the basis of the above considerations, we report our efforts to immobilizing the *n*-propyl sulfamic acid onto hydroxyapatite-encapsulated superparamagnetic γ -Fe₂O₃ nanoparticles, affording high catalytic activity and excellent durability that can be reused properly by external magnet for at least 10 times.

2. Experimental

2.1. Synthesis of nano HAp-encapsulated- γ -Fe₂O₃ [γ -Fe₂O₃@HAp]

Preparation of HAp-encapsulated γ -Fe₂O₃ was carried out according to the previously reported method [39–41]. A mixture of FeCl₂·4H₂O (368 mg, 1.85 mmol) and FeCl₃·6H₂O (1 g, 3.7 mmol) were dissolved in 30 mL deionized water (DW) under Ar atmosphere at r.t., then a 25% NH₄OH solution (10 mL) was added to the resulting solution with vigorous mechanical stirring (700 rpm). A black precipitate of Fe₃O₄ was produced instantly. In order to obtain small and uniform Fe₃O₄ particles, the drop rate of NH₄OH was controlled precisely by a constant dropper, and the drop rate was 1 mL/min. After 15 min, 100 mL of Ca(NO₃)₂·4H₂O (7.95 g, 33.7 mmol) and (NH₄)₂HPO₄ (2.64 g, 20 mmol) solutions adjusted to pH = 11 were added drop-wise to the obtained precipitate over 30 min with mechanical stirring. The resultant milky solution was heated to 90 °C. After 2 h, the mixture was cooled up to r.t and aged overnight. The dark brown precipitate formed was filtered, washed repeatedly with DW until neutral, and air dried under vacuum at r.t. The as-synthesized sample was calcined at 300 °C for 3 h, resulted in a reddish-brown powder (γ -Fe₂O₃@HAp).

2.2. Synthesis of *n*-propylamine covalently supported on HAp-encapsulated- γ -Fe₂O₃ [γ -Fe₂O₃@HAp-Si-(CH₂)₃-NH₂]

A sample of magnetic hydroxyapatite (500 mg) was pre-activated by heating under vacuum for 48 h at 120 °C and suspended in a mixture of 150 mL of dry toluene containing a stoichiometric amount (92 mg, 0.5 mmol) of 3-aminopropyltrimethoxysilane. The used amounts of this agent

were estimated by assuming two hydroxyl groups per formula of phosphate. The mixture was refluxed under Ar atmosphere at 100 °C for 48 h. The product was separated by filtration, washed with ethanol, and dried under vacuum for 24 h at 50 °C after soxhlet extraction by hot ethanol to give the solid surface bonded amine group at a loading 0.75 mmol g⁻¹ (calculated by the back-titration analysis).

2.3. Synthesis of *n*-propylsulfamic acid supported on HAp-encapsulated- γ -Fe₂O₃ [γ -Fe₂O₃@HAp-Si-(CH₂)₃-NHSO₃H]

The [γ -Fe₂O₃@HAp-Si-(CH₂)₃-NH₂] (0.75 mmol g⁻¹, 10 g) was allowed to react with chlorosulfonic acid (ClSO₃H) (8.6 mmol, 1 g) at r.t over 30 min. The mixture was mechanically stirred vigorously for 6 h until HCl gas evolution was stopped. The resulted magnetic nanoparticles were separated by an external magnet device and were washed with hot ethanol and deionized water until neutral to remove the unreacted chlorosulfonic acid. It washed twice with diethyl ether (100 mL) and then dried under vacuum at r.t to give the corresponding solid surface bonded *n*-propylsulfamic acid group (Scheme 1) at a loading 0.7 mmol g⁻¹ (calculated by TGA, back-titration and ion exchange pH analysis). To ensure that no dissolution happened under reaction conditions, the ratio of Fe₂O₃/HAp (w/w) in Fe₂O₃@HAp was determined based on Fe/Ca (w/w) ratio using energy dispersive X-ray spectroscopy analysis, equal to 0.46. The ratio did not have change before and after reacting with chlorosulfonic acid because the reaction done in room temperature and also with short time.

2.4. pH analysis of [γ -Fe₂O₃@HAp-Si-(CH₂)₃NHSO₃H]

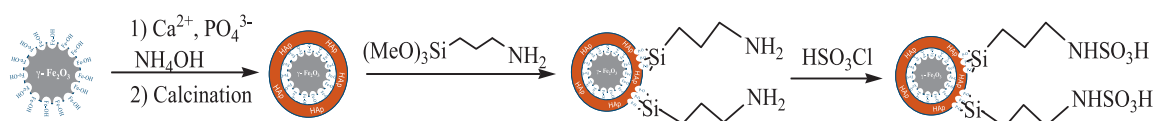
To an aqueous solution of NaCl (1 M, 25 mL) with an initial pH = 5.93, the γ -Fe₂O₃@HAp-Si (CH₂)₃NHSO₃H (50 mg) was added and the resulting mixture stirred for 3 h after which the pH of solution decreased to 2.85. This result confirmed by back-titration analysis of the catalyst: To this analysis we added 10 mL of a standard 0.1 M sodium hydroxide solution to 100 mg of the synthesized catalyst in a 50 mL Erlenmeyer flask. Excess amount of the base was neutralized by addition of a standard 0.1 M HCl solution to the equivalence point of titration. The required volume of HCl to this point was 9.3 mL. This is equal to a loading 0.7 mmol NHSO₃H g⁻¹.

2.5. Elemental analysis of [γ -Fe₂O₃@HAp-Si-(CH₂)₃NHSO₃H]

For confirmation of catalyst loading obtained from several above methods, elemental analysis was carried out using a Vario EL-III CHNOS elemental analyzer. Characterization of new magnetic catalyst showed 3.65% C and 2.36% S (= 0.76 mmol NHSO₃H g⁻¹). Results confirmed other data.

2.6. General procedure for one-pot synthesis of quinolines

γ -Fe₂O₃@HAp-Si-(CH₂)₃NHSO₃H (10 mg, 0.7 mol%) was added to a mixture of a 2-aminoaryl ketone (1 mmol) and a ketone having α -methylene group (1.2 mmol) and allowed to stirred at r.t (Scheme 2). The progress was monitored by TLC (see Table 1). The catalyst separated by a magnet device, washed with diethyl ether and dried to reuse in the next run. All isolated products gave sat-



Scheme 1. Preparation of the γ -Fe₂O₃@HAp-Si-(CH₂)₃-NHSO₃H.

Table 1
Catalyzed Friedlander reaction of 2-aminoaryl ketones with ketones.

| Entry | R ¹ /R ² | R ³ /R ⁴ | Product 3 | Time (h) | Yield ^a (%) | TON ^b | TOF (h ⁻¹) ^c |
|-------|-----------------------------------|---|------------------|----------|------------------------|------------------|-------------------------------------|
| a | -H/-CH ₃ | -CH ₃ /-CO ₂ Et | | 3 | 93 | 132.8 | 44.3 |
| b | -H/-CH ₃ | -CH ₃ /-COCH ₃ | | 3 | 95 | 135.7 | 45.2 |
| c | -H/-CH ₃ | -CH ₂ (CH ₂) ₂ CO- | | 1.5 | 96 | 137.1 | 91.4 |
| d | -H/-C ₆ H ₅ | -CH ₃ /-CO ₂ Et | | 3 | 94 | 134.3 | 44.8 |
| e | -H/-C ₆ H ₅ | -CH ₃ /-CO ₂ Me | | 3 | 95 | 135.7 | 45.2 |
| f | -H/-C ₆ H ₅ | -CH ₃ /-CO ₂ ^t Bu | | 3 | 93 | 132.8 | 44.3 |
| g | -H/-C ₆ H ₅ | -CH ₃ /-COCH ₃ | | 3.5 | 91 | 130 | 37.1 |
| h | -H/-C ₆ H ₅ | -CH ₂ (CH ₂) ₂ CO- | | 3 | 93 | 132.8 | 44.3 |
| i | -H/-C ₆ H ₅ | -CH ₂ C(CH ₃) ₂ CH ₂ CO- | | 3 | 93 | 132.8 | 44.3 |
| j | -H/-C ₆ H ₅ | -(CH ₂) ₄ - | | 3 | 96 | 137.1 | 45.7 |
| k | -H/-C ₆ H ₅ | -(CH ₂) ₃ - | | 3 | 95 | 135.7 | 45.2 |

Table 1 (Continued)

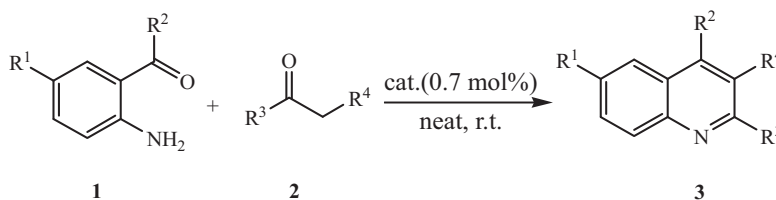
| Entry | R ¹ /R ² | R ³ /R ⁴ | Product 3 | Time (h) | Yield ^a (%) | TON ^b | TOF (h ⁻¹) ^c |
|-------|------------------------------------|---------------------------------------|------------------|----------|------------------------|------------------|-------------------------------------|
| l | -Cl/-C ₆ H ₅ | -CH ₃ /-CO ₂ Et | | 1.5 | 97 | 138.6 | 92.4 |
| m | -Cl/-C ₆ H ₅ | -CH ₃ /-CO ₂ Me | | 1.5 | 97 | 138.6 | 92.4 |

Reaction conditions: 2-aminoaryl ketone (1 mmol), carbonyl compound (1.1 mmol), γ -Fe₂O₃@HAp-Si-(CH₂)₃-NHSO₃H (10 mg, 0.7 mol%); quenched after mentioned times. For entry (a) the catalyst was recycled and used for 10 cycles (each of them 2 h) with conversion of >85% in all the cycles.

^a The yields refer to pure isolated products characterized by spectral data.

^b Turnover number (average number of product molecules produced per mole of the catalyst).

^c Turnover frequency (turnover number per time).



Scheme 2. γ -Fe₂O₃@HAp-Si-(CH₂)₃-NHSO₃H catalyzed Friedlander reaction.

Table 2

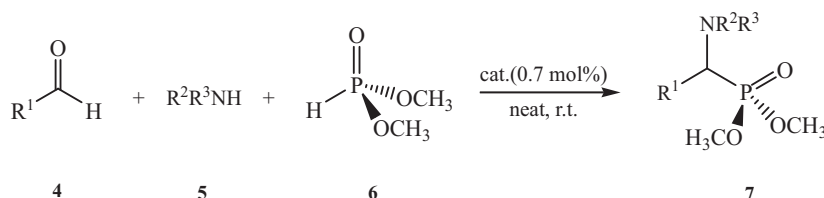
Friedlander annulation of 2-amino acetophenone and ethylacetoacetate with different catalysts. Reaction conditions: free solvent, r.t., 0.7 mol% catalyst quenched after 3 h.

| Entry | Catalyst | Yield |
|-------|--|-------|
| 1 | No catalyst | N.R. |
| 2 | γ -Fe ₂ O ₃ @HAp | N.R. |
| 3 | γ -Fe ₂ O ₃ @HAp-SO ₃ H | 57% |
| 4 | Homogeneous sulfamic acid | 17% |
| 5 | γ -Fe ₂ O ₃ @HAp-Si-(CH ₂) ₃ NHSO ₃ H | 93% |

satisfactory spectral data (¹H NMR and ¹³C NMR) and compared with those reported in literature [42].

2.7. General procedure for one-pot synthesis of α -aminophosphonate

γ -Fe₂O₃@HAp-Si-(CH₂)₃-NHSO₃H (10 mg, 0.7 mol%) was added to a mixture of aldehyde (1.0 mmol) and amine (1.0 mmol) at r.t (Scheme 3). The mixture was stirred for 10 min and then dimethylphosphite (1.1 mmol) was added. Reaction proceeds at r.t and completion of the reaction indicated by TLC. Then the catalyst was separated by an external magnet, washed with diethyl ether and dried to reuse. The organic phase was evaporated under reduced pressure and all isolated products gave satisfactory spectral data (¹H NMR and ¹³C NMR) compared with those reported in literature (Table 3) [43].



Scheme 3. One-pot three-component procedure for the synthesis of α -aminophosphonates catalyzed by γ -Fe₂O₃@HAp-Si-(CH₂)₃-NHSO₃H.

3. Results and discussion

Magnetic sulfamic acid heterogenized on hydroxyapatite-encapsulated γ -Fe₂O₃ was synthesized according to the procedure shown in Scheme 1. γ -Fe₂O₃ nanocrystallites are commonly synthesized by coprecipitation of ferrous (Fe²⁺) and ferric (Fe³⁺) ions in a basic aqueous solution followed by thermal treatment. We employed the coprecipitation approach because basic aqueous media permit subsequent crystallization of the hydroxyapatite phase and lead to coating of the γ -Fe₂O₃ nanoparticles by hydroxyapatite (γ -Fe₂O₃@HAp). The nanocrystallites of γ -Fe₂O₃@HAp were reacted with 3-aminopropyltrimethoxysilane to produce an organic-inorganic hybrid. Then, this synthesized hybrid was affected by chlorosulfonic acid. After 6 h the brown powder washed by deionized water and diethyl ether and dried under vacuum which led to the formation of the *n*-propylsulfamic acid moiety functionalized core-shell catalyst (γ -Fe₂O₃@HAp-Si-(CH₂)₃-NHSO₃H). [γ -Fe₂O₃@HAp-Si-(CH₂)₃-NHSO₃H] nanocrystallites were fully characterized by TEM (Fig. 1a and b), SEM (Fig. 1c), TGA (Fig. 1d), FTIR (Fig. 1e), XRD (Fig. 1f) and ion exchange pH-analysis. Due to the superparamagnetic nature of its core, nuclear magnetic resonance (NMR) technique could not be used to confirm surface modification of the Si-(CH₂)₃NHSO₃H. Instead, acid-base back titration and FTIR were used to characterization of the organic functional group. The loading of sulfamic acid moiety on surface was determined by means of ion-exchange pH-analysis and TGA analysis. In FTIR, charac-

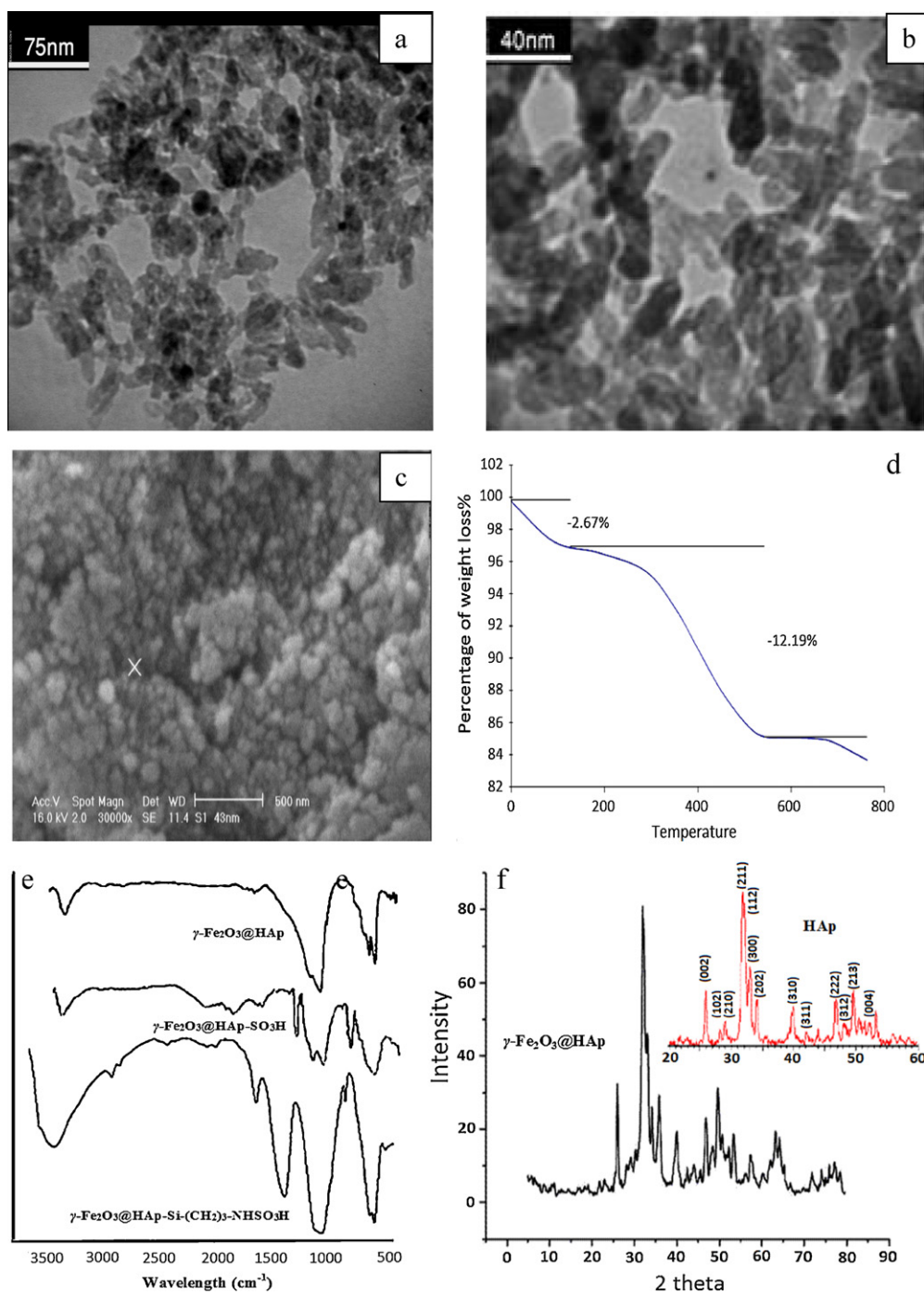


Fig. 1. (a–b) TEM micrograph, (c) SEM image, (d) TGA diagram, (e) FTIR spectrum and (f) XRD spectrum of the $\gamma\text{-Fe}_2\text{O}_3\text{@HAp-Si-(CH}_2\text{)}_3\text{-NHSO}_3\text{H}$.

teristic absorption bands due to the bending vibration mode of O–P–O surface phosphate groups in the hydroxyapatite shell were observed at 567 and 607 cm^{-1} which were in overlap with Fe–O stretching. Also the stretching of P–O bond appeared at 1041 cm^{-1} overlapped with S–O stretching peak. The S=O stretching band of sulfamic group appeared at 1377 cm^{-1} . The stretching and out of plane bending of acidic O–H group observed at $2700\text{--}3500$ and 815 cm^{-1} , respectively. $\gamma\text{-Fe}_2\text{O}_3\text{@HAp}$ was subject to the further structural characterization with XRD, Fig. 1f. Diffraction peaks at around 18.4° , 30.2° , 35.7° , 43.6° , 56.2° and 63.1° corresponding to the (111), (220), (311), (400), (440) and (511) are readily recognized from the XRD pattern. The observed diffraction peaks agree well with that of the tetragonal structure of $\gamma\text{-Fe}_2\text{O}_3$ (1999

JCPDS file No. 13-0458). No other phase except the maghemite is detectable [8]. Both the scanning electron microscopy (SEM) and TEM showed that the encapsulated nanoparticles were present as uniform particles and the size of encapsulated nanoparticles was less than 50 nm . The obtained histogram (Fig. 2) confirmed the fact that the size of distribution for 75 observed nanoparticles was a narrow normal one with a 69 nm average value and a 2.1 nm standard deviation. The theoretical curve of standard distribution from our studies (Fig. 2) was calculated by means of origin program.

Quantitative determination of the functional group loaded on the surface of $\gamma\text{-Fe}_2\text{O}_3\text{@HAp-Si-(CH}_2\text{)}_3\text{-NHSO}_3\text{H}$ was performed utilizing thermo-gravimetric analysis (TGA) and a loading of $0.73 \pm 0.01\text{ mmol g}^{-1}$ was obtained. The analysis showed two

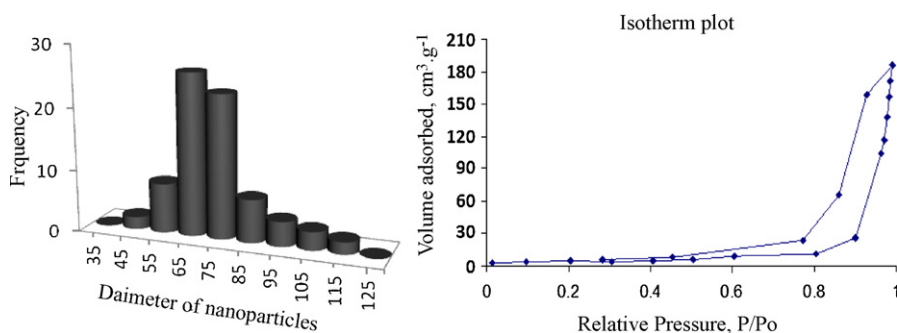


Fig. 2. The histogram of $\gamma\text{-Fe}_2\text{O}_3\text{@HAp-Si-(CH}_2\text{)}_3\text{-NHSO}_3\text{H}$ nanoparticles sizes by means of the SEM image (left) and the isotherm plot of $\gamma\text{-Fe}_2\text{O}_3\text{@HAp-Si-(CH}_2\text{)}_3\text{-NHSO}_3\text{H}$ (right).

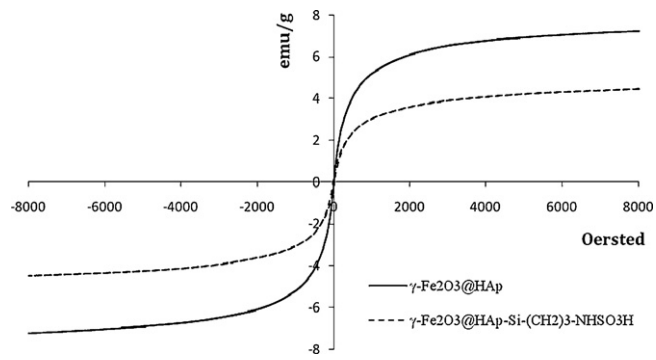


Fig. 3. VSM curve of $\gamma\text{-Fe}_2\text{O}_3\text{@HAp}$ (line) and $\gamma\text{-Fe}_2\text{O}_3\text{@HAp-Si-(CH}_2\text{)}_3\text{-NHSO}_3\text{H}$ (dotted line) at r.t.

peaks. First peak appears due to desorption of the water (centered at 110 °C). This is followed by a second peak at 425 °C, corresponding to loss of the organic spacer group. These results are in agreement with those of ion-exchange pH and back-titration analyses.

Nitrogen adsorption–desorption isotherms are shown in Fig. 2 and reveal that the adsorption–desorption process is not reversible. This is a result of the hysteresis loops due to capillary condensation. The surface area was calculated using BET method, and a value of 122 m² g⁻¹ was found for synthetic hydroxyapatite coated magnetic nanoparticle ($\gamma\text{-Fe}_2\text{O}_3\text{@HAp}$). This average was reduced to 97 m² g⁻¹ for *n*-propyl sulfamic acid functionalized hydroxyapatite coated magnetic nanoparticle powder ($\gamma\text{-Fe}_2\text{O}_3\text{@HAp-Si-(CH}_2\text{)}_3\text{-NHSO}_3\text{H}$). The synthetic powder showed a type (IV) nitrogen adsorption–desorption isotherm (Fig. 2).

It is of great importance that the core/shell material should possess sufficient magnetic and superparamagnetic properties for its practical applications. Magnetic hysteresis measurements for

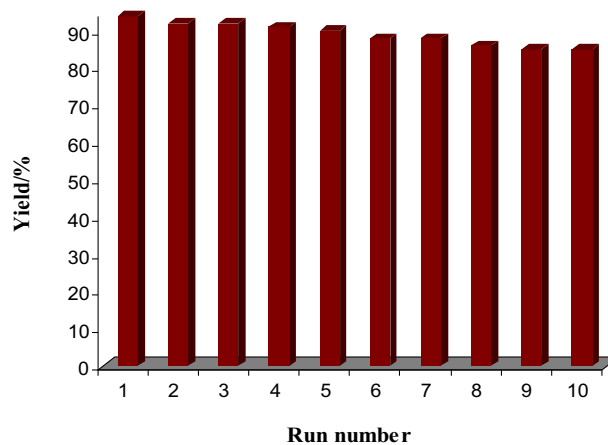


Fig. 5. The recycling experiment of catalyst in friedlander reaction for entry a; carried out at r.t for 3 h.

the $\gamma\text{-Fe}_2\text{O}_3\text{@HAp}$ and $\gamma\text{-Fe}_2\text{O}_3\text{@HAp-Si-(CH}_2\text{)}_3\text{-NHSO}_3\text{H}$ nanoparticles were done in an applied magnetic field at r.t, with the field sweeping from –8000 to +8000 Oersted. As shown in Fig. 3, the M (H) hysteresis loop for the samples was completely reversible, showing that the nanoparticles exhibit superparamagnetic characteristics. The hysteresis loops of them reached saturation up to the maximum applied magnetic field. The magnetic saturation values of the $\gamma\text{-Fe}_2\text{O}_3\text{@HAp}$ and $\gamma\text{-Fe}_2\text{O}_3\text{@HAp-Si-(CH}_2\text{)}_3\text{-NHSO}_3\text{H}$ are 7.24 and 4.49 emu g⁻¹ at r.t, respectively. Lower magnetic saturation of latter nanoparticles can be explained by the influence of the functional group. Both particles showed high permeability in magnetization and their magnetization was sufficient for magnetic separation with a conventional magnet (Fig. 4). The reversibility in hysteresis loop confirms that no aggregation impose to the nanoparticles in the magnetic fields.



Fig. 4. Catalyst ability to effective recovery at the end of reactions.

Catalysis 1: The polysubstituted quinolines are common structural motifs in a wide range of biologically active compounds including antimalaria, antitumor and antibacterial agents [44]. The Friedlander annulation (condensation followed by a cyclodehydration between 2-aminoaryl ketone and a second carbonyl compound including a reactive methylene group) has attracted considerable

attention from the view point of combinatorial chemistry [42] and is one of the simplest and easiest methods for the synthesis of quinolines skeleton. Generally, this reaction is carried out by refluxing an aqueous or an alcoholic solution of reactants in the presence of an acid or base at high temperature. However, the classic Friedlander reaction or modified procedures have significant downsides

Table 3
Catalyzed α -aminophosphonates syntheses.

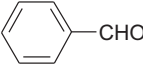
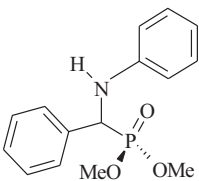
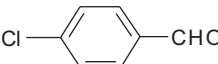
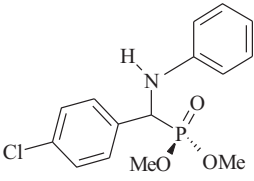
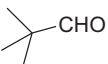
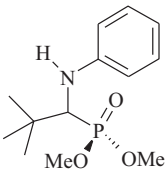
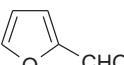
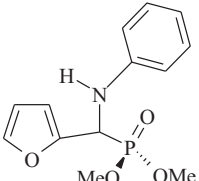
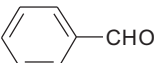
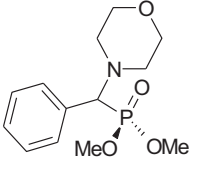
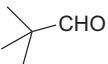
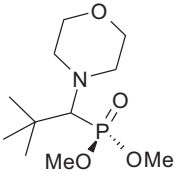
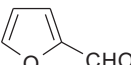
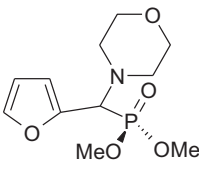
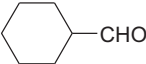
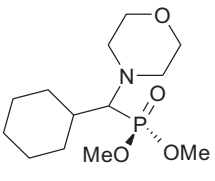
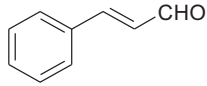
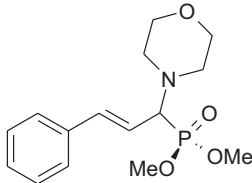
| Entry | Substrate 4 | Time (min) | Product 7 | Yield ^a (%) | TON | TOF (h ⁻¹) |
|-------|---|------------|---|------------------------|-------|------------------------|
| a |  | 40 |  | 95 | 135.7 | 203.5 |
| b |  | 60 |  | 94 | 134.3 | 134.3 |
| c |  | 60 |  | 94 | 134.3 | 134.3 |
| d |  | 35 |  | 97 | 138.6 | 237.6 |
| e |  | 45 |  | 94 | 134.3 | 179.1 |
| f |  | 60 |  | 94 | 134.3 | 134.3 |
| g |  | 35 |  | 98 | 140 | 240 |
| h |  | 45 |  | 94 | 134.3 | 179.1 |

Table 3 (Continued)

| Entry | Substrate 4 | Time (min) | Product 7 | Yield ^a (%) | TON | TOF (h ⁻¹) |
|-------|---|------------|---|------------------------|-------|------------------------|
| i |  | 40 |  | 95 | 135.7 | 203.5 |

Reaction conditions: aldehyde (1 mmol), amine (1 mmol), dimethylphosphite (1.1 mmol), γ -Fe₂O₃@HAp-Si-(CH₂)₃-NH₂SO₃H (10 mg, 0.7 mol%); quenched after mentioned times. For entry (a) the catalyst was recycled and used for 10 cycles (each of them 1 h) with conversion of >90% in all the cycles.

^a The yields refer to pure isolated products characterized by spectral data.

such as low yields, long reaction time, harsh reaction conditions, difficulties in workup and the use of stoichiometric and/or relatively expensive catalysts. Moreover, the main disadvantage of almost all existing methods is that the catalysts are destroyed in the workup and cannot be recovered and reused, which do not conform to environmental standards. Consequently, the development of water stable acidic catalysts for quinoline synthesis is quite desirable. On the basis of the optimal conditions established (0.7 mol% γ -Fe₂O₃@HAp-Si-(CH₂)₃-NH₂SO₃H, air, r.t), we examined the reaction of 2-aminoaryl ketones with various ketones in aqueous medium. As shown in Scheme 2 the reactions proceed smoothly and corresponding quinolines could be obtained in high yields.

At the end of the reaction, to determine the applicability of catalyst recovery, we decanted the vessel by use of an external magnet and remained catalyst was washed with diethyl ether to remove residual product, dried under vacuum and reused in a subsequent reaction. The reaction in entry a resulted in the corresponding quinoline **3a** in 93% isolated yield. In 10 consecutive runs, the conversion stayed with no detectable loss, higher than 85%. To contradiction any contribution of homogeneous catalysis, we tested the reaction leached (after 8 min from the beginning and removal of catalyst) and observed that the reaction did not complete even after 24 h. This clearly confirmed that no active species were present in the supernatant.

We have found that no special handling precaution regarding exposure to air/moisture is needed to be taken in use of γ -Fe₂O₃@HAp-Si-(CH₂)₃-NH₂SO₃H. Table 2 compares new magnetic interphase catalyst with other analogues.

Catalysis 2: Due to their biological activities, phosphonate-containing molecules received much attention in organic syntheses [45]. The utilities of α -aminophosphonates as HIV protease [46], EPSP synthase [47], plant growth regulators [48], anti-thrombotic agents [49], as well as peptidases and proteinases [50] are well documented. α -Aminophosphonates have many biological effects and medicinal importance [51] and therefore many procedures for the synthesis of them have been developed, especially, the nucleophilic addition of phosphates to imines is of the most convenient methods, which is usually promoted by the base [52], Brønsted [53], or variety of Lewis acids [54,55]. However, all of these methods have limitations due to the hygroscopic properties of imines which cause them not to be sufficiently stable for isolation. Using Lewis acids as catalysts and dialkylphosphite and trialkylphosphite as phosphorous reagents, this conversion can proceed in smooth rate. The common used catalysts have some drawbacks for example, reactions require a long time and when starting from aliphatic amines, reactions give non-characterizable products [56]. Additionally, some of these catalysts are either expensive or somewhat difficult to prepare. In many cases the acids were trapped by the basic nitrogen and the reaction require stoichiometric amounts of Lewis acids. These afforded the use of heterogeneous catalysts. Some limitations of the previous methods consist of: harsh

Table 4

The one-pot three-component coupling reaction of benzaldehyde, aniline and dimethylphosphite in the presence of different catalysts. Reaction conditions: free solvent, r.t, 0.7 mol% catalyst quenched after 40 min.

| Entry | Catalyst | Yield |
|-------|--|-------|
| 1 | No catalyst | N.R. |
| 2 | γ -Fe ₂ O ₃ @HAp | 42% |
| 3 | γ -Fe ₂ O ₃ @HAp-SO ₃ H | 68% |
| 4 | Homogeneous sulfamic acid | 21% |
| 5 | γ -Fe ₂ O ₃ @HAp-Si-(CH ₂) ₃ NH ₂ SO ₃ H | 95% |

reaction conditions like inert atmosphere or long time, no reaction with secondary amines and low yields [57–60]. To overcome the drawbacks mentioned above, especially from the standpoint of green chemistry, there is a need to introduce a high flexible way for the synthesis of α -aminophosphonates. With this aim, we tested one-pot three-component procedure for the synthesis of α -aminophosphonates by use of our magnetic inorganic-organic hybrid catalyst, γ -Fe₂O₃@HAp-Si-(CH₂)₃-NH₂SO₃H. One-pot three-component reactions are very attractive since they significantly lower the cost of the synthetic routes as well as reducing the amount of waste and solvents. In the presence of 0.7 mol% of γ -Fe₂O₃@HAp-Si-(CH₂)₃-NH₂SO₃H, the three component coupling reaction involving carbonyl compounds, amines and dialkylphosphite successively proceeded smoothly at r.t to afford the corresponding α -aminophosphonate. Reusability test of the catalyst was also performed successfully in all of 10 recycle runs. Comparison of catalytic efficiencies presents in Table 4.

4. Conclusion

The preparation and characterization of *n*-propyl sulfamic acid covalently supported on hydroxyapatite-encapsulated magnetic nanoparticles was described. Synthesized material acts as a powerful and “green” heterogeneous interphase catalyst for preparation of substituted quinolines and α -aminophosphonates derivatives. We believe that most of the interesting supported organic acid catalysts reported previously have harmful ingredients for human and environment. Hydroxyapatite is found in teeth and bones within the human body. Thus, it is commonly uses as a filler to replace amputated bone or as a coating to promote bone in growth into prosthetic implants. It contains more than 60% of mammalian hard tissues and in addition it has unique biocompatibility feature among phosphate groups. One of the reasons to use of this biocompatible material as catalyst support was that it has no pollution and is in the context of “green chemistry”. This can make our new magnetic catalyst distinct from all of its present analogues. Besides, this new magnetic catalyst has higher activity in comparison with γ -Fe₂O₃@HAp-SO₃H, due to its far catalytic active sites from solid surface and therefore less steric hindrance and less mass transport limitations. The present method requires remarkably small

amounts of non-toxic and green (environmentally friendly) [γ -Fe₂O₃@HAp-(CH₂)₃-NH₂SO₃H] as catalyst (0.7 mol%). The recovered catalyst was recycling in subsequent runs without observation significant decrease in activity even after 10 runs. For example, the reaction of 2-aminoacetophenone and ethylacetoacetate gave substituted quinoline (Table 1, entry a) in sequenced 10 runs (Fig. 5). The mild reaction conditions, excellent yields, operational simplicity, practicability, applicability to various substrates, product purity and therefore cost efficiency are of advantages of this protocol. Besides that, the new catalyst can be effectively reused. With regard to observed satisfactory catalytic properties, it is expected that it can be potential substitute for some commercial catalysts.

Acknowledgements

Prof. Dr. M. Yalpani is thanked for language correction and further assistance in the preparation of the manuscript. The authors sincere thanks go out to Dr. G. Khalili for his kind cooperation for the CHNOS elemental analysis.

Appendix A. Supplementary data

Supplementary data associated with this article can be found, in the online version, at doi:10.1016/j.molcata.2010.12.004.

References

- [1] P.D. Stevens, G. Li, F. Fan, M. Yen, Y. Gao, Chem. Commun. (2005) 4435.
- [2] W. Teunissen, A.A. Bol, J.W. Geus, Catal. Today 48 (1999) 329.
- [3] T.-J. Yoon, W. Lee, Y.-S. Oh, J.-K. Lee, New J. Chem. 27 (2003) 227.
- [4] H. Yoon, S. Ko, J. Jang, Chem. Commun. (2007) 1468.
- [5] H.-H. Yang, S.-Q. Zhang, X.-L. Chen, Z.-X. Zhuang, J.-G. Xu, X.-R. Wang, Anal. Chem. 76 (2004) 1316.
- [6] D. Lee, J. Lee, H. Lee, S. Jin, T. Hyeon, B.M. Kim, Adv. Synth. Catal. 348 (2006) 41.
- [7] C.Ó. Dálaigh, S.A. Corr, Y. Gun'ko, S.J. Connon, Angew. Chem. Int. Ed. 46 (2007) 4329.
- [8] Y. Zhang, Z. Li, W. Sun, C. Xia, Catal. Commun. 10 (2008) 237.
- [9] Z.C. Zhang, L.M. Zhang, L. Chen, L.G. Chen, Q.H. Wan, Biotechnol. Prog. 22 (2006) 514.
- [10] A. Corma, H. Garcia, Chem. Rev. 103 (2003) 4307.
- [11] G.A. Somorjai, K. McCrea, Appl. Catal. A: Gen. 222 (2001) 3.
- [12] B.W. Wojciechowski, A. Corma, Catalytic Cracking, Catalysts Kinetics and Mechanisms, Marcel Dekker, New York, 1984.
- [13] H.U. Blaser, E. Schmidt, Asymmetric Catalysis on Industrial Scale: Challenges Approaches and Solutions, Wiley-VCH, Weinheim, 2004.
- [14] E.N. Jacobsen, A. Pfaltz, H. Yamamoto (Eds.), Comprehensive Asymmetric Catalysis, Springer, Heidelberg, 1999.
- [15] S.V. Malhotra, Methodologies in Asymmetric Catalysis, vol. 880, ACS, Orlando, FL, 2004.
- [16] R. Noyori, Angew. Chem. Int. Ed. 41 (2002) 2008.
- [17] K.B. Sharpless, Angew. Chem. Int. Ed. 41 (2002) 2024.
- [18] E.N. Jacobsen, W. Zhang, A.R. Muci, J.R. Ecker, L. Deng, J. Am. Chem. Soc. 113 (1991) 7063.
- [19] P.T. Anastas, M.M. Kirchhoff, Acc. Chem. Res. 35 (2002) 686.
- [20] M. Poliakoff, J.M. Fitzpatrick, T.R. Farren, P.T. Anastas, Science 297 (2002) 807.
- [21] A. Abad, P. Concepcio, A. Corma, H. Garcia, Angew. Chem. Int. Ed. 44 (2005) 4066.
- [22] A. Corma, H. Garcia, Chem. Rev. 102 (2002) 3837.
- [23] A. Corma, H. Garcia, Adv. Synth. Catal. 348 (2006) 1391.
- [24] B. Cornils, W.A. Herrmann, P. Panster, S. Wieland, Applied Homogeneous Catalysis with Organometallic Compounds, Wiley/VCH, Weinheim, 1996, p. 576.
- [25] K.K. Bando, K. Soga, K. Kunimori, H. Arakawa, Appl. Catal. A: Gen. 175 (1998) 1.
- [26] K. Yuzaki, T. Yarimizu, S. Ito, K. Kunimori, Catal. Lett. 47 (1997) 3.
- [27] H.T. Ma, Z.Y. Yuan, Y. Wang, X.H. Bao, Surf. Interface Anal. 32 (2001) 224.
- [28] A.J. Sandee, J.N. Reek, P.C. Kamer, P.W. Van Leeuwen, J. Am. Chem. Soc. 123 (2001) 8468.
- [29] T. Tago, T. Hanaoka, P. Dhupatemiya, H. Hayashi, M. Kishida, K. Wakabayashi, Catal. Lett. 64 (2000) 27.
- [30] O.G. Da Silva, E.C. da Silva Filho, M.G. da Fonseca, L.N.H. Arakaki, C. Airoidi, J. Colloid Interface Sci. 302 (2006) 485.
- [31] J. Portier, J.H. Choy, M.A. Subramanian, J. Inorg. Mater. 3 (2001) 581.
- [32] A. Stein, B.J. Melde, R.C. Schroden, Adv. Mater. 12 (2000) 1403.
- [33] A.-H. Lu, E.-L. Salabas, F. Schüth, Angew. Chem. Int. Ed. 46 (2007) 1222.
- [34] Y. Gao, in: C.S. Kumar (Ed.), Biofunctionalization of Magnetic Nanoparticles Biofunctionalization of Nanomaterials, Wiley-VCH, Weinheim, 2005, p. 72.
- [35] G. Schmid, Nanoparticles, From Theory to Application, Wiley-VCH, Weinheim, 2004, p. 434.
- [36] R.A. Lee, D.S. Donald, Tetrahedron Lett. 38 (1997) 3857.
- [37] D. Bogdal, M. Lukasiewicz, J. Pielichowski, A. Miciak, Sz. Bendnarz, Tetrahedron 59 (2003) 649.
- [38] S. Laurent, D. Forge, M. Port, A. Roch, C. Robic, L. Vander Elst, R.N. Muller, Chem. Rev. 108 (2008) 2064.
- [39] Y. Zhang, Y. Zhao, C. Xia, J. Mol. Catal. A: Chem. 306 (2009) 107.
- [40] Y. Zhang, C. Xia, Appl. Catal. A: Gen. 366 (2009) 141.
- [41] L. Ma'mani, M. Sheykhan, A. Heydari, M. Faraji, Y. Yammini, Appl. Catal. A: Gen. 377 (2010) 64.
- [42] J. Akbari, A. Heydari, H.R. Kalhor, S. Azizian Kohan, J. Comb. Chem. 12 (2010) 137.
- [43] L. Ma'mani, A. Heydari, R.K. Shiroodi, Curr. Org. Chem. 13 (2009) 758.
- [44] R. Engel, J.I. Cohen, Synthesis of Carbon-Phosphorus Bonds, 2nd ed., CRC Press, 2003.
- [45] B. Stowasser, K.-H. Buda, L. Jian-Qi, A. Peyman, D. Ruppert, Tetrahedron Lett. 33 (1992) 6625.
- [46] J.A. Sikorski, M.J. Miller, D.S. Braccolino, D.G. Cleary, S.D. Corey, I.L. Font, K.J. Gruys, C.Y. Han, K.C. Lin, P.D. Pan-Segrau, J.E. Ream, D. Schnur, A. Shah, M.C. Walker, Phosphorus Sulfur Silicon Relat. Elem. 76 (1993) 115.
- [47] L. Maier, H. Spoerri, Phosphorus Sulfur Silicon Relat. Elem. 61 (1991) 69.
- [48] J.H. Meyer, P.A. Barlett, J. Am. Chem. Soc. 120 (1998) 4600.
- [49] D.J. Miller, S.M. Hammond, D. Anderluzzi, T.D.H. Bugg, J. Chem. Soc. Perkin Trans. 1 (1998) 131.
- [50] T. Yokomatsu, Y. Yoshida, S. Shibuya, J. Org. Chem. 59 (1994) 7930.
- [51] A.N. Pudovik, Dokl. Akad. Nauk SSSR 83 (1952) 865.
- [52] K.A. Petrov, V.A. Chauzov, T.S. Erokhina, Usp. Khim. 43 (1974) 2045.
- [53] S.S. Bhagat, A.K. Chakraborti, J. Org. Chem. 72 (2007) 1263, and reference cited therein.
- [54] A.S. Paraskar, A. Sudalai, Arkivoc 10 (2006) 183.
- [55] R. Ghosh, S. Maiti, A. Chakraborty, D. Maiti, J. Mol. Chem. A 53 (2004) 210.
- [56] B. Kaboudin, R. Nazari, Tetrahedron Lett. 42 (2001) 8211.
- [57] S. Chandrasekhar, S. Jaya Prakash, V. Jagadeshwar, C. Narsihmulu, Tetrahedron Lett. 42 (2001) 5561.
- [58] A. Smahi, A. Solhy, R. Tahir, S. Sebti, J.A. Mayoral, J.I. Garcia, J.M. Fraile, M. Zahouily, Catal. Commun. 9 (2008) 2503.
- [59] M. Zahouily, A. Elmakssoudi, A. Mezdar, A. Rayadh, S. Sebti, Catal. Commun. 8 (2007) 225.
- [60] K. Sukata, Bull. Chem. Soc. Jpn. 60 (1987) 3820.